Antiviral Research 168 (2019) 51–60

Contents lists available at ScienceDirect

Antiviral Research

journal homepage: www.elsevier.com/locate/antiviral

Kinase inhibitors tyrphostin 9 and rottlerin block early steps of rabies virus cycle

Zoé Lama, Yves Gaudin, Danielle Blondel, Cécile Lagaudrière-Gesbert*

Institute for Integrative Biology of the Cell (I2BC), CEA, CNRS, Université Paris-Sud, Université Paris-Saclay, 91198, Gif-sur-Yvette cedex, France

ARTICLE INFO

Keywords:
Rabies virus (RABV)
Rottlerin
Tyrphostin 9
Entry inhibitor
Transcription inhibitor

ABSTRACT

Rabies virus (RABV) is a neurotropic virus that causes fatal encephalitis in humans and animals and still kills up to 59,000 people worldwide every year. To date, only preventive or post-exposure vaccination protects against the disease but therapeutics are missing. After screening a library of 80 kinases inhibitors, we identified two compounds as potent inhibitors of RABV infection: tyrphostin 9 and rottlerin. Mechanism of action studies show that both inhibitors interfere with an early step of viral cycle and can prevent viral replication. In presence of tyrphostin 9, the viral entry through endocytosis is disturbed leading to improper delivery of viral particles in cytoplasm, whereas rottlerin is inhibiting the transcription, most likely by decreasing intracellular ATP concentration, and therefore the replication of the viral genome.

1. Introduction

Rabies is caused by Rabies virus (RABV) an enveloped, negative-stranded, RNA virus that belongs to *Lyssavirus* genus of the *Rhabdoviridae* family. This disease remains a substantial burden on public health by causing fatal encephalitis and killing up to 59,000 people worldwide every year (Hampson et al., 2015). This mortality mainly concerns developing countries where access to prevention and prophylactic treatment is limited. The post-exposure prophylaxis, based on vaccination and passive immunization with rabies immunoglobulin, is effective only when received prior to the onset of the disease. To date there is no treatment once symptoms develop (Jackson, 2014) and rabies remains always fatal. Chemicals able to target viral steps could provide with new insights into RABV biology and pave the way to the characterization of valuable antivirals compounds.

The viral cycle of RABV begins with receptor-mediated endocytosis of the virus, followed by a low-pH-induced membrane fusion process catalyzed by the glycoprotein (G) which results in the release of the ribonucleoprotein (RNP) into the cytoplasm (Albertini et al., 2012). The RNP comprises the helical nucleocapsid (the genome encapsidated by the nucleoprotein N) associated with the RNA dependent RNA polymerase (L) and its cofactor the phosphoprotein (P). Once released in the cytosol, the RNP serves as a template for transcription and replication that are catalyzed by the L–P polymerase complex. These processes occur within viral factories (Lahaye et al., 2009), called Negri bodies (NBs), which have the properties of membraneless liquid organelles (Nikolic et al., 2017). During transcription, a positive–strand leader RNA and five capped and polyadenylated mRNAs are synthesized. Translation will provide the N protein necessary to encapsidate nascent antigenomes and genomes synthesized through the replication process. The resulting nucleocapsids containing full-length antigenome-sense RNA, serve as templates for the synthesis of viral genomic RNA (Albertini et al., 2011). The neo-synthesized genomes either serve as templates for secondary transcription or are condensed and assembled with the matrix protein M and G proteins to allow budding of neo-synthesized virions at a cellular membrane.

Many aspects of RABV replication are still not completely understood, including the roles of cellular factors in the virus life cycle. Cellular kinases are key actors involved in the regulation of signal transduction pathways, including those promoting antiviral cellular defenses as well as those likely regulating RABV proteins functions. Along this line, phosphorylation of the viral protein N by Casein Kinase II (CKII) is known to promote the processes of RABV transcription and replication (Yang et al., 1999) (Wu et al., 2002). Phosphorylation of the phosphoprotein P by PKC modulates the nucleocytoplasmic distribution of the different isoforms of this viral protein and therefore allows the rabies virus to respond and adapt to the cellular environment (Moseley et al., 2007). Furthermore, the phosphoprotein P is phosphorylated on serines 63 and 64 by a unique protein kinase, not yet identified, which appears to be selectively packaged within the mature virion suggesting an important role in the life cycle of RABV (Gupta et al., 2000).

In the present study, we aimed to investigate the antiviral properties

* Corresponding author.
E-mail address: cecile.lagaudriere-gesbert@u-psud.fr (C. Lagaudrière-Gesbert).

https://doi.org/10.1016/j.antiviral.2019.04.014
Received 31 January 2019; Received in revised form 7 April 2019; Accepted 29 April 2019
Available online 07 May 2019
0166-3542/

of a library of 80 kinase inhibitors. We identified two compounds, tyrphostin 9 and rottlerin, to be potent inhibitors that can suppress RABV replication. Further investigations showed that tyrphostin 9 inhibited viral fusion by preventing endosome acidification, whereas rottlerin inhibited the replication of RABV by shutting down RNA synthesis through ATP deprivation.

2. Materials and methods

2.1. Cells and viruses

N2A cells (mouse neuroblastoma), U373-MG cells (human glioblastoma astrocytoma) and BSR cells, a clone from BHK21 (Baby Hamster Kidney) were grown in Dulbeco's modified eagle medium (DMEM) supplemented with 10% FCS (fetal calf serum), 100 U/ml penicillin and 100U/ml streptomycin. To establish BSR cell lines expressing fluorescent proteins, BSR were stably transfected by Lipofectamine 2000 (Invitrogen), and antibiotics-resistant single cell colonies were selected by G418 (Sigma-Aldrich) and expanded into cell lines. BSR stable cell lines were maintained in medium containing 0.4 mg/ml G418. Mouse primary neurons were obtained from JM Peyrin (Université Pierre-et-Marie Curie, CNRS UMR 7102, Paris) as described (Deleglise et al., 2013).

The SAD-B19 and CVS 11 (Challenge virus standard - “French”) strains of rabies virus (Ugolini, 2010) and VSV (Mudd-Summer strain, Indiana serotype) were grown in BSR cells. The SAD (B19)-GFP was provided by Dr. T. Mebatsion.

2.2. Plasmids

The plasmid YFP-GalT was kindly provided by Dr Mavrakis (Ward et al., 2001). The plasmid pEGFP encoding GFP was obtained from Clontech.

2.3. Antibodies and reagents

The rabbit polyclonal anti-P (5.2) antibody, the mouse monoclonal anti-P (25C2) antibody, the mouse monoclonal anti-N (81C4) antibody and the mouse monoclonal anti-G (30AA5) antibody were previously described (Lahaye et al., 2009). The rabbit polyclonal anti-PKCδ (C-20) was obtained from Santa Cruz Biotechnology. The mouse monoclonal anti-αtubulin (DM1A) and anti-β3tubulin (T4026) were purchased from Sigma Aldrich. Secondary fluorescent antibodies were purchased from Molecular Probes (Alexa fluor 488, 568 or 647 conjugated) and Cell Signaling (Fluor 800 or Fluor 680 conjugated). The kinase inhibitors library used was the « Screen-Well® Kinase Inhibitor Library » (BML-2832) from Enzo life Science. Cycloheximide, Proteinase K and CCCP (Carbonyl Cyanide 3-Chlorophenylhydrazone) were from Sigma Aldrich. Ribavirin was obtained from Abcam.

2.4. Screening of inhibitors

BSR cells were seeded at 2.5×10^4 per well in 96 well plates the day before infection. They were infected with SAD (B19)-GFP strain (MOI 3) in medium containing 10 µM of each inhibitor. At 16 h post-infection (hpi), cells were harvested with Cell Dissociation Solution (Sigma). The GFP fluorescence was determined using a BD Accuri C6 Flow Cytometer. Experimental MOIs were precisely determined using the equation $MOI = -\ln [p (0)]$ where p (0) is the proportion of non-infected cells and compared to that in presence of DMSO which was normalized to 1.

2.5. Cell viability assays

Two assays were used to evaluate cell viability upon treatments with the drugs. The MTT [3-(4,5-dimethylthiazol-2yl)-2,5-diphenyltetrazolium bromide] assay was performed using Sigma reagents according to the manufacturer's instructions. The propidium iodide (PI) uptake staining was followed by flow cytometry on BD Accuri C6 Flow Cytometer. The viability was expressed as the ratio of the corresponding absorbance (MTT) or fluorescence (PI) to that of DMSO treated cells taken arbitrarily as 100% (samples done in triplicate).

2.6. Immunofluorescence staining and confocal microscopy

Cells monolayers grown on glass coverslip were fixed for 20 min with 4% PFA (paraformaldehyde) and permeabilized for 15 min with 0.1% Triton X-100 in PBS (phosphate-buffered saline). Cells were incubated with the indicated primary antibodies for 1 h at RT, washed and incubated for 1 h with Alexa fluor conjugated secondary antibodies. Following washing, cells were mounted with Immu-Mount (Shandon) containing DAPI (4,6 diamidino-2-phenylindole) to stain nuclei. Images were captured in sequential recording mode using a Leica SP8 confocal microscope (63X oil-immersion objective). Confocal stacks were treated with ImageJ Software.

2.7. Detection of viral mRNA and genomic RNA by RT-qPCR

Quantitative real-time RT-PCR was performed as described previously (Nikolic et al., 2016). Briefly, total RNA was extracted with Nucleospin RNA II kit (Macherey Nagel, France) and 2 µg of RNA was used for the first strand cDNA synthesis by reverse transcription with AffinityScript QPCR cDNA synthesis kit (Agilent Technologies, USA). First strand cDNA was synthesized using oligo-(dT) primers (200 ng) for mRNA quantification and forward primer of viral P gene (5′- CTT GAG ATG GCC GAA GAG AC) for viral genomic RNA (gRNA) quantification. Quantitative real-time PCR was performed on a Mx3000P apparatus (Stratagene, USA) in a total volume of 20 µl containing the first strand cDNA template, 200 nM of each primer and 1x Mesa green QPCR master mix plus solution (Eurogentec, France). Standard curves for the housekeeping gene glyceraldehyde-3-phosphate dehydrogenase (GAPDH) were obtained by using serial dilutions of human genomic DNA. Forward and reverse primers for GAPDH were 5′- ACA GCC TCA AGA TCA TCA GC (f) and 5′- TCT TCT GGG TGG CAG TGA T (r), respectively. The plasmid pCW278 containing the cDNA of RABV-CVS-N2C genome was used to establish standard curves for quantification of P mRNAs and calculate the amplification efficiency. Primers used for RABV-P gene were 5′- CTT GAG ATG GCC GAA GAG AC (f) and 5′- ACG ATT GGA ACA GGA GGT TG (r). Each amplification reaction was carried out in triplicate with the following conditions: an initial denaturation at 95 °C for 10 min, 40 cycles of 95 °C for 10 s, 60 °C for 30 s and 72 °C for 10 s. The uniqueness and sizes of PCR products were checked by agarose gel electrophoresis. BSR cells mock-infected were used as controls.

2.8. Small interfering RNA (siRNA) transfection

A pool of 4 siRNAs targeting PKCδ were purchased from GE Healthcare (ON-TARGET plus human PRKCD siRNA SMART pool and ON-TARGET plus non-targeting pool). Cells (U373-MG) were seeded at 5×10^4 per well in 24 well plates the day before infection. Transient transfections with a final siRNA concentration of 25 nM were performed using Dharmafect reagent according to the manufacturer's instructions. Cells were infected (CVS MOI 3) and treated with or without rottlerin (3 µM) 48 h post-transfection. Western-blot analysis was performed 24 h post-infection.

2.9. Western blot analysis

Cells were harvested in citric saline buffer (135 mM KCl, 15 mM citric acid), washed in PBS and lysed in cold lysis buffer (50 mM Tris-

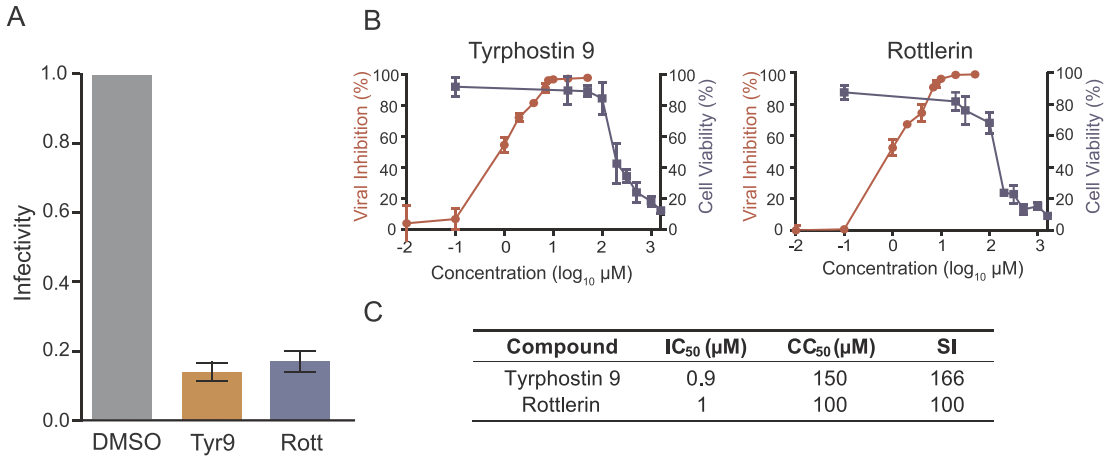

Compound	IC_{50} (µM)	CC_{50} (µM)	SI
Tyrphostin 9	0.9	150	166
Rottlerin	1	100	100

Fig. 1. Identification of kinase inhibitors tyrphostin 9 and rottlerin with anti-RABV activity. (A) BSR cells seeded in 96-well plates were infected with SAD-GFP virus at MOI 3 and treated with each compound (3 µM) or DMSO as control. 16 hpi, infectivity was determined by counting the number of cells expressing GFP using a flow cytometer. Data depict the mean with standard deviation for three experiments performed in triplicate. (B). Determination of cytotoxicity (MTT assay) and dose-response curves of tyrphostin 9 (left panel) and rottlerin (right panel) for inhibiting SAD-GFP infection. For MTT assay, BSR cells were incubated with various concentrations of the respective agents or DMSO as control for 16 h prior to the assay. For dose-dependent inhibition assay, BSR cells were infected with SAD-GFP virus at MOI 3 and treated with various concentrations of the respective agents or DMSO as control. Cells expressing GFP were counted using a flow cytometer 16 hpi. Errors bars indicate standard deviation ($n = 3$). (C) IC50, CC50 and SI values for tyrphostin 9 and rottlerin.

HCl, pH 7.5, 150 mM NaCl, 0.5% NP40 supplemented with a cocktail of protease inhibitors (Roche)) for 30 min on ice. Lysates were clarified by centrifugation at 15,000 × *g* for 20 min at 4 °C. Proteins were separated on 12% SDS-PAGE and transferred onto a Nitrocellulose membrane. The membrane was blocked with 5% skimmed milk in TBS, incubated with the primary antibody of interest and with the appropriate Fluor 800 or Fluor 680-conjugated secondary antibody (Cell Signaling). The membrane was scanned with the Odyssey infrared imaging system (LI-COR, Lincoln, NE) at a wavelength of 700 or 800 nm.

2.10. Binding and internalization assays

Cells (BSR) were seeded at 3×10^5 per well in 24 well plates on glass coverslip the day before infection. CVS virus (MOI 80) was bound to the cells on ice for 1 h. The inoculum was washed away with cold PBS. For binding assay, cells were fixed with 4% PFA in PBS for 15 min. For internalization assay, preheated medium (37 °C) supplemented or not with inhibitors was added and the cells were transferred at 37 °C. At the desired time, cells were washed with cold PBS and fixed in 4% PFA. Alternatively, cells were treated with Proteinase K (0.5 mg/ml) for 20 min at room temperature, then washed with cold PBS containing 0.2% BSA and 1 mM PMSF for 15 min on ice and fixed in 4% PFA. All sample were processed for immuno-staining with anti-G antibody and immunofluorescence analysis. DAPI was used to stain the nuclei. Images were captured in sequential recording mode using a Leica SP8 confocal microscope (63X oil-immersion objective). For each field (about 40 cells/field), 35 planes were acquired by confocal microscopy and a max intensity Z-projection was done using ImageJ. Quantifications of G-containing spots were performed using the image toolbox of MatLab software. Each spot was considered as a single virion and the total number of spots in the image was divided by the number of nuclei in the field.

2.11. pHrodo red dextran assay

BSR cells were seeded at 4×10^5 per well in 12 well plates the day before. They were pre-treated with tyrphostin 9 (3 µM) or NH_4Cl (20 mM) for 2.5 h at 37 °C before addition of the pHrodo Red dextran (final concentration of 50 µg/ml) for 20 min at 37 °C. Cells were harvested with Cell Dissociation Solution supplemented with 20 mM NH_4Cl and the fluorescence was determined by flow cytometry using a BD Accuri C6 Flow Cytometer.

2.12. Measurement of intracellular ATP

BSR cells were seeded at 1×10^4 per well in 96 well plates the day before and grown in DMEM supplemented with 10 mM Galactose and penicillin/streptomycin. Cells were incubated in triplicate with a concentration range of rottlerin, CCCP (or DMSO) during 16 h at 37 °C. Measurement of intracellular ATP was performed using the Mitochondrial ToxGlo assay from Promega according to the manufacturer's instructions.

2.13. Data analysis

All dose–response curves, IC_{50} and CC_{50} values and statistical analysis were determined using Prism software GraphPadPrism4 (San Diego, CA).

3. Results

3.1. Identification of tyrphostin 9 and rottlerin as rabies virus inhibitors

We used an immunofluorescence-based assay to screen a commercially available collection of 80 inhibitors of mammalian Ser/Thr and Tyr kinases for anti-RABV activity. Only two compounds significantly neutralized infectivity of the SAD-GFP strain (Fig. 1A). Tyrphostin 9 and rottlerin exerted a dose-dependent inhibition of viral infection (Fig. 1B). The 50% inhibitory concentrations (IC_{50}) were similar for the two compounds, 0.9 µM for tyrphostin 9 and 1 µM for rottlerin (Fig. 1C). To ensure that the anti-RABV activity was not due to cellular cytotoxicity, we used an MTT assay to assess cell viability (Fig. 1B). We found that the 50% cellular cytotoxicity (CC_{50}) was greater than 100 µM for each inhibitor (150 µM for tyrphostin 9 and 100 µM for rottlerin). The selective index (SI, the ratio of the CC50 to the IC50) for tyrphostin 9 was 166, while that for rottlerin was 100 (Fig. 1C). Further experiments were conducted at the concentration of 3 µM unless mentioned.

3.2. Tyrphostin 9 and rottlerin effectively reduce RABV infection in vitro

To confirm the anti-RABV activities of tyrphostin 9 and rottlerin, we

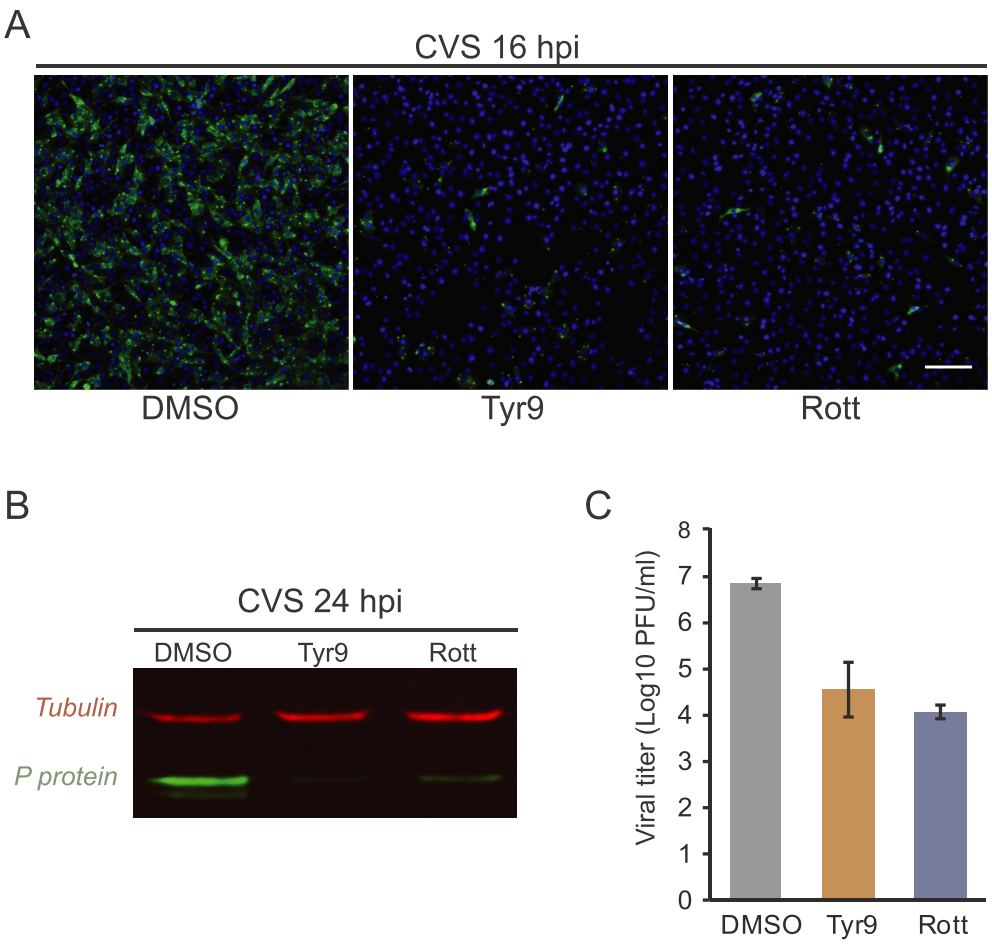

Fig. 2. Tyrphostin 9 and rottlerin inhibit RABV CVS strain. (A) BSR cells grown on glass coverslips were infected with CVS strain at MOI of 3 for 16 h in presence of 3 μM of tyrphostin 9 (Tyr9), rottlerin (Rott) or DMSO as control. Cells were fixed and stained with mouse anti-N antibody followed by incubation with Alexa-488 donkey anti-mouse IgG. DAPI was used to stain the nuclei. Scale bars correspond to 100 μm. (B) Western-blot analysis of viral P protein at 24 hpi in presence of tyrphostin 9 (Tyr9), rottlerin (Rott) or DMSO as control in BSR cells infected with CVS virus (MOI of 3). Detection of α-tubulin was included as loading control. (C) Virus titers of BSR cells supernatants. Cells were infected with CVS virus (MOI of 3) for 16 h in presence of 3 μM of tyrphostin 9 (Tyr9), rottlerin (Rott) or DMSO as control. The virus titers were quantified by plaque assay. Data represent averages of titers from 3 independent experiments. The error bars indicate standard deviations.

examined whether they can block infection of another RABV strain. BSR cells were infected with the CVS strain and viral protein expression was analyzed 16 hpi. Fig. 2A shows a strong decreased number of cells staining positively for N protein in presence of tyrphostin 9 or rottlerin when compared with the mock treated RABV infected cells. Consistent with these findings, P protein was highly expressed in DMSO-treated cells but not or barely detectable in the tyrphostin 9 or rottlerin-treated cells when analyzed by western-blotting (Fig. 2B). To further determine the effects on viral growth, the virus release in the culture supernatants was quantified by plaque assay 16 hpi. As shown in Fig. 2C, the viral titers in the control (DMSO), tyrphostin and rottlerin treated cells were 6.85 ± 0.09, 4.56 ± 0.58 and 4.08 ± 0.15 $\log_{10}$ PFU/ml, respectively. In presence of both inhibitors the production of progeny virus is thus reduced by more than two orders of magnitude.

The antiviral efficacy of the two compounds was then evaluated in different cell lines. We examined the effect of tyrphostin 9 and rottlerin on RABV infection in BSR, N2A (murine neuroblastoma) and U373-MG (human glioblastoma astrocytoma) cell lines (Fig. 3A). Cells were infected with SAD-GFP strain and treated with noncytotoxic concentrations of tyrphostin 9 and rottlerin. Even though in a lesser extent in N2A, in all three cell lines tested the infectivity was highly decreased in cultures treated with tyrphostin 9 (by a factor ~25 in BSR and U373-MG cells at 5 μM). Regarding rottlerin, a similar antiviral activity was observed in BSR and U373-MG cells at 3 and 5 μM. As tyrphostin 9, this compound was less efficient in N2A cells with only a reduction factor of ~3. The antiviral efficacy was also evaluated in primary neurons. At 16 hpi, infection with the CVS strain in mouse primary neurons was analyzed by immunofluorescence and microscopy using an anti-P antibody and counterstaining with anti-β3 tubulin to identify neurons. The infection was effectively prevented in presence of either tyrphostin 9 or rottlerin at 5 μM (Fig. 3B). In these primary cells, tyrphostin 9 and rottlerin exhibited also a strong inhibitory effect on SAD-GFP infection at 5 μM with a drop of the infectivity by a factor 10 and 6, respectively (Fig. 3C). At lower concentration (3 μM) rottlerin was ineffective and tyrphostin 9 inhibitory effect was moderate (Fig. 3C).

Altogether these results indicate that anti-RABV tyrphostin 9 and rottlerin inhibitory effects on RABV infection are not restricted to a single cell type. They are able to block different viral strains; however depending on the cell type and the strain, the IC_{50} may vary.

3.3. Tyrphostin 9 and rottlerin inhibit an early stage of the rabies virus life cycle

To define which step of the viral replication cycle is affected by the two inhibitors, a time-of-drug-addition assay was performed to assess whether they inhibit RABV replication at an early or late stage. BSR cells were infected with CVS virus and at various time points post-infection, were treated with DMSO or the inhibitor. Both tyrphostin 9 and rottlerin elicited an inhibitory effect on infectivity when they were applied to the RABV-infected culture up to 4–7 hpi. At later time points, the antiviral activity was attenuated and reached a plateau (infectivity reduced by a factor ~1,5), suggesting that tyrphostin 9 and rottlerin prevent an early step of the viral cycle (Fig. 4A).

We then investigated whether tyrphostin 9 and rottlerin affected viral entry. In these experiments ammonium chloride (NH_4Cl) was used as an early stage reference compound which prevents acidification of endosome and therefore the fusion step required for the release of RNP in the cytosol (Johannsdottir et al., 2009). To analyze binding to cells, CVS virions were allowed to bind to BSR cells on ice for 1 h in presence of the compounds. The unbound viruses were washed away and the

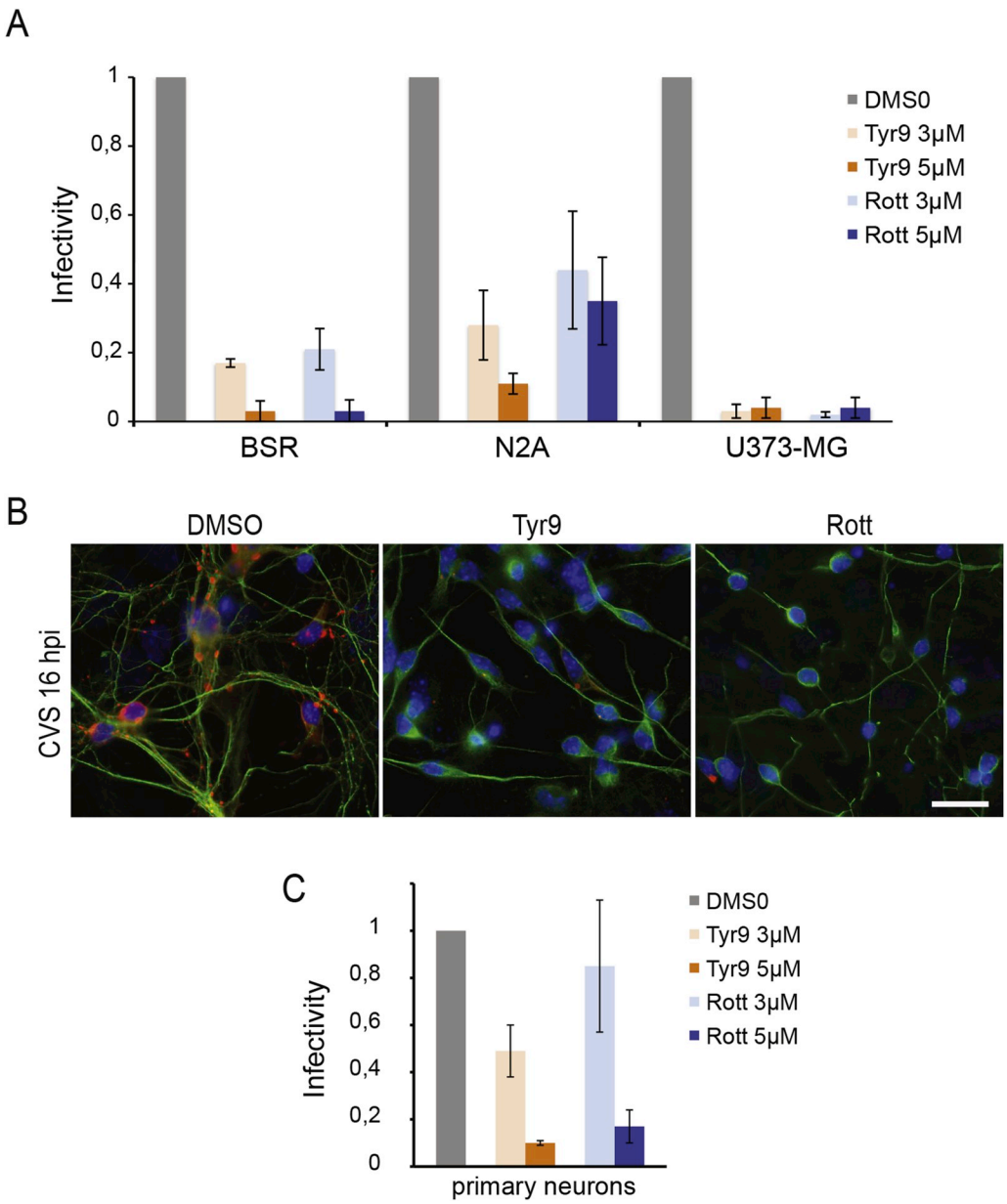

Fig. 3. Tyrphostin 9 and rottlerin block RABV infection in different cell types. (A) U373-MG cells, N2A cells and BSR cells were infected with SAD-GFP virus at MOI of 3 for 16 h in presence of 3 or 5 μM of tyrphostin 9 (Tyr 9), rottlerin (Rott) or DMSO as control. Infectivity was determined by counting the number of cells expressing GFP using a flow cytometer. Data depict the mean with standard deviation for experiments performed in triplicate. (B) Primary neurons were infected with CVS virus at MOI of 3 in presence of 5 μM of tyrphostin 9 (Tyr 9), rottlerin (Rott) or DMSO as control. At 16 hpi, cells are analyzed by epifluorescent-microscopy after co-staining with the mouse anti-β3 tubulin (green) and rabbit anti-P (red) followed by incubation with Alexa-488 and Alexa-568. DAPI (blue) was used to stain the nuclei. The scale bar corresponds to 30 μm. (C) Primary neurons were infected with SAD-GFP virus at MOI of 3 in presence of 3 or 5 μM of tyrphostin 9 (Tyr 9), rottlerin (Rott), or DMSO as control. 16 hpi, infectivity was determined by counting the number of cells expressing GFP using a flow cytometer. Errors bars indicate standard deviation ($n = 3$).

remaining cell-associated particles were detected with an anti-G antibody before analysis by immunofluorescence and confocal microscopy. We observed small G-containing fluorescent spots which were assimilated to single viral particles (Fig. 4B). The number of cells in the field was determined by counting the number of nuclei (stained by DAPI). This allowed the determination of the average number of viral particles bound per cell which was similar in all tested conditions (Fig. 4C). This indicated that none of the inhibitors affected viral adsorption at the cell surface.

To analyze how rapidly cell-bound RABV particles were internalized, CVS viruses were allowed to bind to BSR cells on ice for 1 h and then the cells were warmed up at 37 °C for different time (0–4 h). Each inhibitor was added during adsorption and kept all over the experiment. Virions present at the cell surface were observed and counted after fixation and G-immunostaining on non-permeabilized cells. The quantification of G-containing spots per cell showed that the fraction of virions present at the cell surface decreased over time in the same extent in all conditions (Fig. 4D left panel). To analyze internalization of RABV particles, we performed a protease digestion (to remove cell-surface bound virions) at different times post warming, prior to fixation, permeabilization and G-immunostaining. Different profiles were observed. In DMSO or rottlerin treated cells, 40% of G-containing spots were resistant to proteinase K after 3 min and this number decreased over time. Their disappearance after 1 h is indicative of efficient fusion with endosomal membrane and release of RNP in the cytosol. In cells exposed to tyrphostin 9, the entry was significantly delayed with only 15% of G-containing spots internalized after 3 min. They increased over time to reach 60% after 4 h at 37 °C, likely due to accumulation in endosomal compartments. Indeed, similar results were observed in presence of NH_4Cl which blocks acidification (Fig. 4B and D right panels). These observations indicated that rottlerin has a post-entry effect whereas tyrphostin 9 acts earlier by preventing RNP release in the cytosol.

3.4. *Tyrphostin 9 prevents endosomal acidification and disrupts Golgi complex*

Tyrphostin 9 is mainly described and used as an inhibitor of the PDGF receptor tyrosine kinase activity (Bilder et al., 1991). However in our screen none of the other compounds acting on PDGF receptor

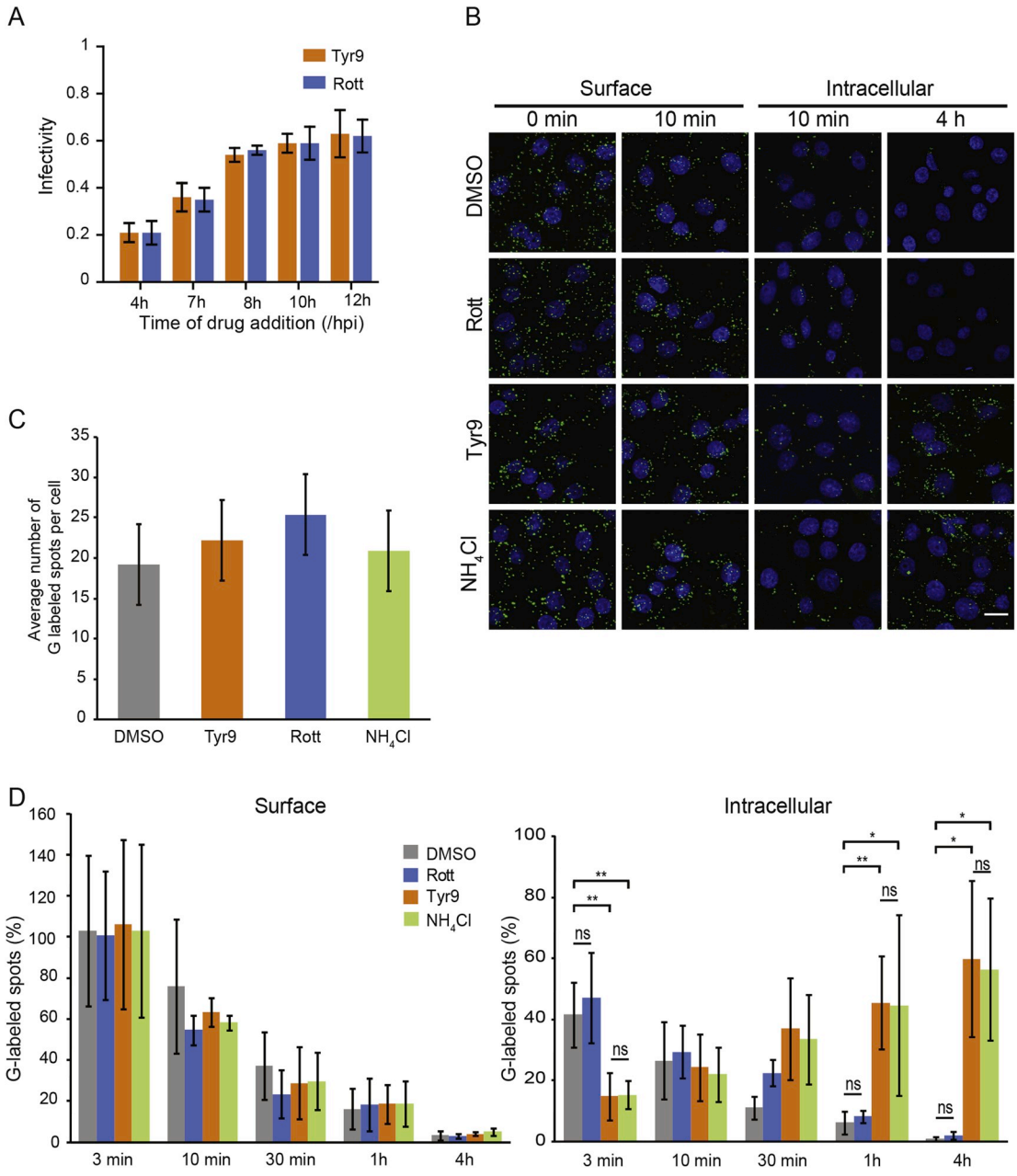

Fig. 4. Tyrphostin 9 and rottlerin inhibit the early stages of the RABV viral cycle. (A) BSR cells were infected with CVS strain at a MOI of 3 for 16 h and, at different time points during the course of infection, treated with 3 μM of tyrphostin 9, rottlerin or DMSO as control. Cells were fixed and stained with mouse anti-N antibody followed by incubation with Alexa-488 donkey anti-mouse IgG. Infectivity was determined by counting the number of cells expressing viral N protein. Data depict the mean with standard deviation for experiments performed in triplicate. (B–D) BSR cells were exposed to RABV (MOI 80) and the viruses were allowed to bind to the cells at 4 °C for 1 h (Adsorption). After washing, warm medium containing 3 μM of tyrphostin 9, rottlerin, 20 mM NH_4Cl or DMSO as control was added and samples were shifted to 37 °C for the indicated time. Prior to fixation, cells were treated or not with Proteinase K to distinguish internalized (intracellular) from external (surface) particles. Cells were fixed, stained with anti-G antibody (green) and DAPI (blue), and imaged using confocal microscopy. (B) 2D projections of 10 focal planes. (C) Quantification of viral adsorption (cell bound viruses at 4 °C). The number of G-labeled spots per cells was quantified with MatLab. Each time point represents the average of four independent experiments in triplicate. Error bars show standard deviation. (D) Quantification of cell surface bound and internalized viruses after incubation at 37 °C. The percentage of viral dots was quantified with MatLab. Results are normalized to viral Adsorption. Each time point represents the average of four independent experiments in triplicate. Error bars show standard deviation. ns, not significant; **, $p < 0.01$; *, $p < 0.05$ (Student's *t*-test).

(Tyrphostin 47, Tyrphostins AG-1295 and AG-1296) (Levitzki and Gazit, 1995) happened to have an inhibitory effect on RABV infection. Therefore, it is unlikely that the mechanism involved in the anti-RABV activity relies on an effect of tyrphostin 9 on the PDGF receptor signaling pathway. Interestingly, tyrphostin 9 has been shown to have a strong influence on the morphology of the Golgi complex (Thyberg, 1998). Therefore, we examined the fate of the Golgi complex in tyrphostin 9 treated cells. As Golgi marker, we used an YFP-tagged version of the N-linked glycoprotein-processing enzyme galactosyltransferase (GalT) that distributes throughout the Golgi stack (Sciaky et al., 1997). In BSR stable cell lines expressing GalT-YFP and exposed to DMSO, the GalT-YFP was localized primarily to perinuclear Golgi structures as expected (Fig. 5A). When acidification of endosomes was impaired by NH_4Cl treatment, the morphology of Golgi was unchanged, whilst tyrphostin 9 caused a dispersion of the Golgi complex that could be observed after 30 min of exposure to the drug. Such an important effect on

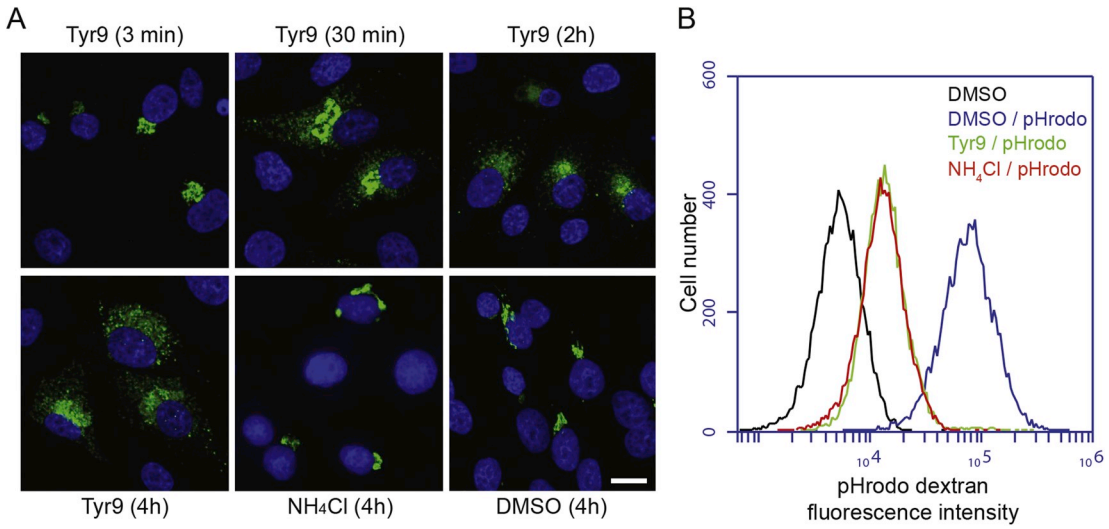

Fig. 5. Tyrphostin 9 disturbs the Golgi compartment and blocks endosomal acidification. (A) BSR- YFP-GalT (green) cells were incubated with tyrphostin 9 (3 μM), NH_4Cl (20 mM) or DMSO. At different time points, cells were fixed and analyzed by confocal microscopy. DAPI (blue) was used to stain the nuclei. Scale bar corresponds to 10 μm. (B) BSR cells were preincubated with tyrphostin 9 (3 μM), NH_4Cl (20 mM) or DMSO for 2.5 h before addition of pHrodo Red dextran. After incubation 20 min, fluorescence intensity was measured using a flow cytometer. Representative composite fluorescence plots of three independent experiments performed in triplicate are shown.

Golgi complex might have consequences on the regulation of intracellular membrane traffic and could impair the maturation of endosomes. To test this hypothesis, we examined the uptake of dextran coupled to the pH-sensitive dye pHrodo Red that displays little fluorescence at neutral pH and fully unquenched fluorescence in acidic environments. We measured that the mean fluorescence intensity in tyrphostin 9 treated cells was lower than that of control cells (DMSO), consistent with the localization of the probe in a non-acidic compartment (Fig. 5B). Cells treated with the endosomal acidification inhibitor NH_4Cl also showed reduced fluorescence. This result supports to the notion that tyrphostin 9 prevents endosome maturation and acidification, and in that way RABV genome release into the host cell.

3.5. Rottlerin inhibits viral RNA synthesis

We have shown that rottlerin inhibits viral life cycle at an early stage but does not affect viral entry. In order to further dissect the stage of viral replication affected by this inhibitor, we investigated whether rottlerin is able to inhibit RNA synthesis.

To determine if rottlerin affects viral transcription, BSR cells were infected with CVS strain and P-mRNA were quantified. The results showed that viral transcription is strongly inhibited in presence of rottlerin (Fig. 6A) as early as 4 hpi. This suggested that primary transcription is affected as genome replication (and therefore secondary transcription) only occurs after ~8hr (Wu et al., 2002).

We also investigated the effect of rottlerin on RNA replication (*ie* genomic RNA synthesis), BSR cells were infected with RABV for 8 h and genomic RNA (gRNA) species were quantified. Compared to results with DMSO control, addition of rottlerin or ribavirin, a known inhibitor of RABV RNA polymerase (Appolinario et al., 2013), decreased the levels of gRNA by more than 60% (Fig. 6B) showing that, as expected from its observed effect on primary transcription, rottlerin prevents viral replication.

Rottlerin effect on viral replication was not related to a putative rottlerin-induced translation inhibition as GFP, transiently expressed in BSR cells after transfection, was only slightly lowered in rottlerin treated cells compared to DMSO control (Fig. 6C). Indeed, such a low impact on cellular translation could not explain the drastic inhibition of RNA replication observed in presence of rottlerin (Fig. 6C).

To confirm that rottlerin affects viral primary transcription, we uncoupled the transcription process from the replication process by inhibiting *de novo* protein synthesis in the infected cells. BSR cells were infected with CVS strain in presence of cycloheximide (CHX) added to the culture medium to completely inhibit protein synthesis and consequently viral replication. Unexpectedly, at 8 hpi in presence of rottlerin or DMSO as control, the phosphoprotein P mRNA levels were similar in the two conditions (Fig. 6D) revealing that rottlerin does not inhibit transcription in presence of CHX.

3.6. siRNA mediated silencing of PKCδ does not prevent RABV replication

Rottlerin is described as an inhibitor of the PKCδ, to determine whether PKCδ could be the cellular kinase mediating the anti-viral activity of rottlerin, we evaluated the effect of siRNA-mediated "knockdown" of PKCδ expression on RABV infection. U373-MG cells were transfected with a pool of four siRNAs specific for PKCδ. This resulted in an effective reduction of PKCδ expression when compared to cells transfected with the non-targeting control, but this treatment did not prevent phosphoprotein P expression upon CVS infection (Fig. 6E), revealing that PKCδ is dispensable for RBAV infection. Therefore, PKCδ is not the cellular target involved in the anti-RABV activity of rottlerin.

3.7. Rottlerin and ATP depletion

Several studies have pointed out that rottlerin can modulate biological events in a PKCδ-independent manner (Soltoff, 2007). Indeed, rottlerin is a mitochondrial uncoupler agent. Its effects on mitochondrial membrane potential correlate with a depletion of the cellular ATP concentration that subsequently inhibits many cellular processes (Kayali et al., 2002) (Tapia et al., 2006). Therefore, we evaluated the effect of rottlerin on cellular ATP content in BSR cells and compared its effects with CCCP, a protonophore that collapses the mitochondria inner membrane potential. Treatment with increasing concentrations of rottlerin or CCCP caused a significant and similar reduction in ATP levels at concentrations above 1 μM for each drug (Fig. 7A). In order to relate the effect of rottlerin on RABV infection with the decline of cellular ATP concentration, we performed further experiments using CCCP to investigate whether this agent could also inhibit infectivity. BSR cells were infected with CVS strain in presence of increasing concentrations of CCCP (or DMSO as control). As observed with rottlerin,

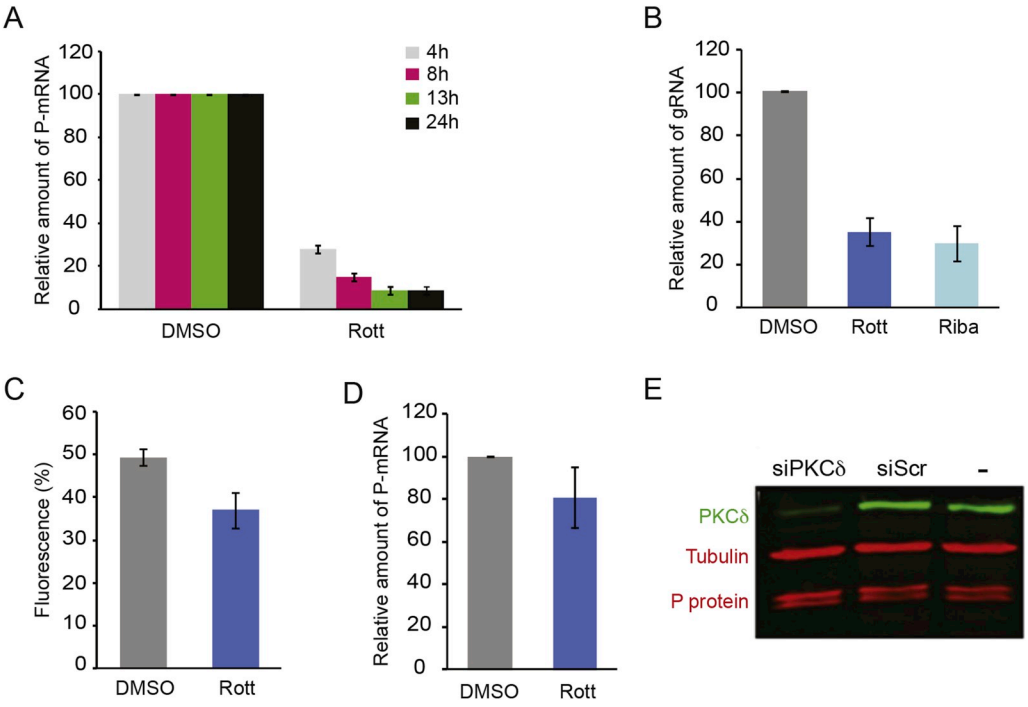

Fig. 6. Rottlerin prevents viral replication. (A) BSR cells were infected with CVS virus at MOI 3 in presence of rottlerin (Rott, 3 μM) or DMSO. At different times post-infection, total RNA was extracted from cells. The relative amount of P mRNA was determined by RT-qPCR and normalized to those of GADPH mRNA as described in Materials and Methods. Mean values and standard deviations of three independent experiments are shown. (B) BSR cells were infected with CVS virus at MOI 3 in presence of rottlerin (Rott, 3 μM), ribavirine (Riba, 8 μM) or DMSO. 8 hpi, total RNA was extracted from cells. The relative amount of genomic RNA was determined by RT-qPCR and normalized to those of GADPH mRNA as described in Materials and Methods. Mean values and standard deviations of three independent experiments are shown. (C) BSR cells were transfected with pcDNA3.1-GFP in presence of rottlerin (3 μM) or DMSO (control). After 48 h, the percentage of GFP positive cells was quantified by flow cytometry. Error bars show standard deviation for two experiments done in triplicate. (D) BSR cells were infected with CVS virus at MOI 3 and in presence of cycloheximide (100 μM) and rottlerin (Rott, 3 μM) or DMSO. 8 hpi, total RNA was extracted from cells. The relative amount of P mRNA was determined by RT-qPCR and normalized to those of GADPH mRNA as described in Materials and Methods. Mean values and standard deviations of three independent experiments are shown. (E) BSR cells were non-transfected (−) or transfected with non-targeting (siScr) or PKCδ-targeting (siPKCδ) siRNA. 48 h post-transfection, cells were infected with CVS virus (MOI of 3) and 20 hpi cell extracts were analyzed by western-blot using anti-PKCδ, anti-P and anti-α-tubulin antibodies.

CCCP caused a dose-dependent inhibition of viral infection with an IC_{50} of 2,5 μM (Fig. 7B). Accordingly, we could observe that viral protein expression was diminished in infected cells treated with CCCP at concentrations as low as 0.1 μM and totally prevented at 5 μM and above (Fig. 7C). No cytotoxicity was observed at up to 5 μM CCCP (Fig. 7B). For comparison purpose, we also performed a time-of-drug-addition assay with CCCP to check whether this agent was preventing an early step of the viral replication cycle. CCCP displayed an inhibitory effect on infectivity when added within the first 8 h of infection mimicking the inhibitory effects of rottlerin on RABV replication (Fig. 7D). These

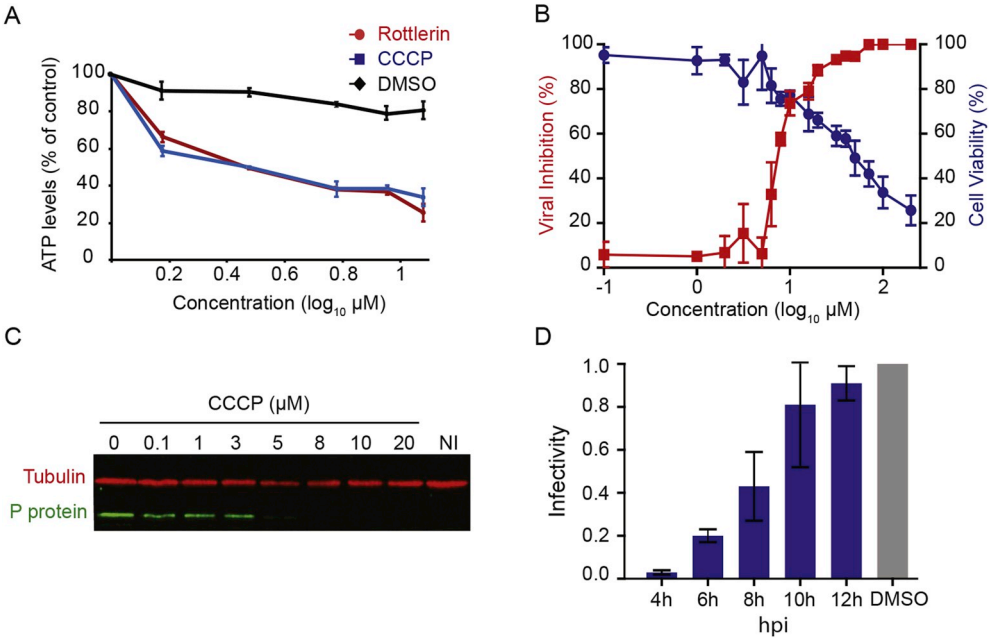

Fig. 7. The mitochondrial uncoupler CCCP inhibits RABV infection. (A) BSR cells were incubated for 16 h with increasing concentrations of CCCP, rottlerin or DMSO as control. Cellular ATP levels were measured using Mitochondrial ToxGlo assay. Data represent averages from 3 independent experiments done in triplicate. The error bars indicate standard deviations. (B) Determination of cell viability (PI uptake) and dose-response curves of CCCP for inhibiting CVS infection. For PI uptake assay, BSR cells were incubated with various concentrations of CCCP (or DMSO as control) for 16 h prior to the assay. For dose-dependent inhibition assay, BSR cells were infected with CVS virus at MOI 3 and treated with various concentrations of CCCP (or DMSO). Cells were fixed and stained with mouse anti-N antibody followed by incubation with Alexa-488 donkey anti-mouse IgG. Infectivity was determined by counting the number of cells expressing viral N. Data depict the mean with standard deviation for three experiments performed in triplicate. (C) BSR cells were treated with a range of CCCP and infected with CVS virus (MOI 3). 16 hpi, cell extracts were analyzed by western-blot using anti-P (green) and anti-α-tubulin (red) antibodies. (D) BSR cells were infected with CVS strain (MOI 3) and, at different time points during the course of infection, treated with 3 μM of CCCP. 16 hpi, cells were fixed and stained with mouse anti-N antibody followed by incubation with Alexa-488 donkey anti-mouse IgG. Infectivity was determined by counting the number of cells expressing viral N protein and compared to that obtained in presence of DMSO which was normalized to 1 (cf Materials and Methods). Data depict the mean with standard deviation for three experiments performed in triplicate.

results indicate that the effects of rottlerin to inhibit RABV replication are most likely related to its ability to act as a mitochondrial uncoupler and reduce ATP levels.

4. Discussion

To date, there are few documented inhibitors for RABV infections and their mechanism of action are not always well characterized. The reported inhibitors include the purine analogue ribavirin (Appolinario et al., 2013) and favipiravir (Banyard et al., 2017) that disrupt efficient virus replication, amantadine that impedes viral release in the cytosol (Superti et al., 1985), a small molecule hit inhibiting PPxY-Host Nedd 4 exhibiting anti-budding activity (Han et al., 2014) and more recently amphibian antimicrobial peptides called dermaseptins (Mechlia et al., 2018) that could possibly reduce attachment and/or entry of virus in target cells and pyrimethamine (Rogée et al., 2018), which inhibits rabies infection *in vitro* through the inhibition of adenosine synthesis. Antiviral drugs for the treatment of RABV infections are urgently needed, since there are currently no antiviral therapies available. Kinases activities being involved in the regulation of major cellular signaling pathways and likely to play important roles in viral infection and replication (Keating and Striker, 2012), we screened kinase inhibitors in an effort to identify those that could block RABV infection. We identified two molecules, tyrphostin 9 and rottlerin, that can each potently inhibit RABV replication (Fig. 1) at different steps of the virus life cycle, impairing cellular entry (Fig. 4) and RNA synthesis (Fig. 6). Both compounds display anti-RABV activities in different cell types, including neurons, the predominantly RABV infected cells (Fig. 3).

Classical known targets of tyrphostin 9 and rottlerin did not explain their antiviral activity against RABV. Tyrphostin 9 has been originally described as selective antagonist of the PDGFR pathway, but the antiviral property of tyrphostin 9 highlighted in the present study is most likely not linked to its effects on PDGFR signaling, since tyrphostin 9 was shown to inhibit PDGFR in the low nanomolar range (Levitzki and Gilon, 1991), whereas inhibition of RABV infection requires micromolar concentrations (Fig. 1B). Along this line, by testing additional pharmacologic inhibitors, we were unable to verify the importance of the PDGFR kinase activity in RABV infection. Instead, our results demonstrate that tyrphostin 9 blocks RABV access to the cellular interior (Fig. 4A) primarily by preventing the maturation of endosomal compartment (Fig. 5B), which is required for the low pH-dependent fusion entry step. Given the disrupting effect of tyrphostin 9 on Golgi complex (Fig. 5A), it is reasonable to hypothesize that tyrphostin 9 might affect the phosphorylation, and therefore the function, of cellular factor(s) involved in vesicular trafficking that remain to be identified. The mechanism through which tyrphostin 9 inhibit other viral infections, such as Influenza A virus (Kumar et al., 2011) or herpes simplex virus (Yura et al., 1995), remains also unclarified as the target could not be identify precisely either.

Antiviral effects have also been reported for rottlerin. It has been shown to inhibit the macropinocytosis dependent viral entry of various viruses, including Kaposi's sarcoma-associated herpesvirus (Raghu et al., 2009) and vaccinia virus (Sandgren et al., 2010). Moreover, combined approaches of rottlerin treatment and siRNA knock-down have revealed that PKCδ promotes HIV and Rift Valley Fever virus replication (Contreras et al., 2012; Filone et al., 2010). The mechanism involved in the anti-RABV effect of rottlerin appears to be different as RABV infection was inhibited in rottlerin-treated cells (Fig. 1), but not in PKCδ knockdown cells (Fig. 6E). Treatment with CCCP inhibited RABV infection as observed following rottlerin treatment. This indicates that depolarization of the mitochondrial membrane potential could be the mechanism underlying rottlerin-mediated inhibition of RABV. Rottlerin mainly targets the synthesis of viral RNA (Fig. 6A and B). To explain this phenomenon, one can hypothesize that the decrease in intracellular ATP caused by rottlerin (or CCCP) either impacts the viral polymerase activity or impairs a cellular kinase activity that is required at early steps of the viral replication. In presence of CHX, this inhibitory effect is not observed (Fig. 6D). This might be related to the blockade of translation that is highly energy-consuming. In this case, the inhibitory effect of rottlerin might be attenuated, the available ATP pool being essentially used for viral transcription.

In conclusion, we have identified two compounds able to block early steps of RABV viral cycle. Their effects on RABV infection *in vitro* is clear, but remains to be investigated *in vivo*. One important issue regarding anti-rabies therapy is efficient drug delivery to the central nervous system that is complicated by the presence of the blood-brain barrier. In this respect, rottlerin is of interest as its neuroprotective effect have already been shown in preclinical animal models of Parkinson disease (Zhang et al., 2007). Given their quite low selectivity (Fig. 1C), tyrphostin 9 and rottlerin are unlikely to be useful antiviral agents themselves, nevertheless our work establishes for the first time the potential utility of kinase inhibitors as post exposure antiviral drugs for Rabies.

Fundings

This work was supported by the Centre National de la Recherche Scientifique.

Acknowledgement

We thank Ahmet Civas for helpful discussions. The present work has benefited from the light microscopy facility of Imagerie-Gif, (http://www.i2bc.paris-saclay.fr), member of IBiSA (http://www.ibisa.net), supported by “France-BioImaging” (ANR-10-INBS-04-01), and the Labex “Saclay Plant Sciences” (ANR-10-LABX-0040-SPS).

References

Albertini, A.A., Baquero, E., Ferlin, A., Gaudin, Y., 2012. Molecular and cellular aspects of rhabdovirus entry. Viruses 4, 117–139. https://doi.org/10.3390/v4010117.

Albertini, A.A., Ruigrok, R.W., Blondel, D., 2011. Rabies virus transcription and replication. In: Advances in Virus Research. Elsevier, pp. 1–22. https://doi.org/10.1016/B978-0-12-387040-7.00001-9.

Appolinario, C.M., Prehaud, C., Allendorf, S.D., de Paula Antunes, J.M.A., Peres, M.G., Lafon, M., Megid, J., 2013. Ribavirin has an in vitro antiviral effect in rabies virus infected neuronal cells but fails to provide benefit in experimental rabies in mice. Virol. Antiviral Res. 2. https://doi.org/10.4172/2324-8955.1000111.

Banyard, A.C., Mansfield, K.L., Wu, G., Selden, D., Thorne, L., Birch, C., Koraka, P., Osterhaus, A.D.M.E., Fooks, A.R., 2017. Re-evaluating the effect of Favipiravir treatment on rabies virus infection. Vaccine. https://doi.org/10.1016/j.vaccine.2017.10.109.

Bilder, G.E., Krawiec, J.A., McVety, K., Gazit, A., Gilon, C., Lyall, R., Zilberstein, A., Levitzki, A., Perrone, M.H., Schreiber, A.B., 1991. Tyrphostins inhibit PDGF-induced DNA synthesis and associated early events in smooth muscle cells. Am. J. Physiol. Cell Physiol. 260, C721–C730. https://doi.org/10.1152/ajpcell.1991.260.4.C721.

Contreras, X., Mzoughi, O., Gaston, F., Peterlin, M.B., Bahraoui, E., 2012. Protein kinase C-delta regulates HIV-1 replication at an early post-entry step in macrophages. Retrovirology 9, 37. https://doi.org/10.1186/1742-4690-9-37.

Deleglise, B., Lassus, B., Soubeyre, V., Alleaume-Butaux, A., Hjorth, J.J., Vignes, M., Schneider, B., Brugg, B., Viovy, J.-L., Peyrin, J.-M., 2013. Synapto-protective drugs evaluation in reconstructed neuronal network. PLoS One 8, e71103. https://doi.org/10.1371/journal.pone.0071103.

Filone, C.M., Hanna, S.L., Caino, M.C., Bambina, S., Doms, R.W., Cherry, S., 2010. Rift Valley fever virus infection of human cells and insect hosts is promoted by protein kinase C epsilon. PLoS One 5, e15483. https://doi.org/10.1371/journal.pone.0015483.

Gupta, A.K., Blondel, D., Choudhary, S., Banerjee, A.K., 2000. The phosphoprotein of rabies virus is phosphorylated by a unique cellular protein kinase and specific isomers of protein kinase C. J. Virol. 74, 91–98. https://doi.org/10.1128/JVI.74.1.91-98.2000.

Hampson, K., Coudeville, L., Lembo, T., Sambo, M., Kieffer, A., Attlan, M., Barrat, J., Blanton, J.D., Briggs, D.J., Cleaveland, S., Costa, P., Freuling, C.M., Hiby, E., Knopf, L., Leanes, F., Meslin, F.-X., Metlin, A., Miranda, M.E., Müller, T., Nel, L.H., Recuenco, S., Rupprecht, C.E., Schumacher, C., Taylor, L., Vigilato, M.A.N., Zinsstag, J., Dushoff, J., on behalf of the Global Alliance for Rabies Control Partners for Rabies Prevention, 2015. Estimating the global burden of endemic canine rabies. PLoS Neglected Trop. Dis. 9, e0003709. https://doi.org/10.1371/journal.pntd.0003709.

Han, Z., Lu, J., Liu, Y., Davis, B., Lee, M.S., Olson, M.A., Ruthel, G., Freedman, B.D., Schnell, M.J., Wrobel, J.E., Reitz, A.B., Harty, R.N., 2014. Small-molecule probes targeting the viral PPxY-host Nedd4 interface block egress of a broad range of RNA

viruses. J. Virol. 88, 7294–7306. https://doi.org/10.1128/JVI.00591-14.
Jackson, A.C., 2014. Recovery from rabies: a call to arms. J. Neurol. Sci. 339, 5–7. https://doi.org/10.1016/j.jns.2014.02.012.
Johannsdottir, H.K., Mancini, R., Kartenbeck, J., Amato, L., Helenius, A., 2009. Host cell factors and functions involved in vesicular stomatitis virus entry. J. Virol. 83, 440–453. https://doi.org/10.1128/JVI.01864-08.
Kayali, A.G., Austin, D.A., Webster, N.J.G., 2002. Rottlerin inhibits insulin-stimulated glucose transport in 3t3-L1 adipocytes by uncoupling mitochondrial oxidative phosphorylation. Endocrinology 143, 3884–3896. https://doi.org/10.1210/en.2002-220259.
Keating, J.A., Striker, R., 2012. Phosphorylation events during viral infections provide potential therapeutic targets. Rev. Med. Virol. 22, 166–181. https://doi.org/10.1002/rmv.722.
Kumar, N., Liang, Y., Parslow, T.G., Liang, Y., 2011. Receptor tyrosine kinase inhibitors block multiple steps of Influenza a virus replication. J. Virol. 85, 2818–2827. https://doi.org/10.1128/JVI.01969-10.
Lahaye, X., Vidy, A., Pomier, C., Obiang, L., Harper, F., Gaudin, Y., Blondel, D., 2009. Functional characterization of Negri bodies (NBs) in rabies virus-infected cells: evidence that NBs are sites of viral transcription and replication. J. Virol. 83, 7948–7958. https://doi.org/10.1128/JVI.00554-09.
Levitzki, A., Gazit, A., 1995. Tyrosine kinase inhibition: an approach to drug development. Science 267, 1782–1788. https://doi.org/10.1126/science.7892601.
Levitzki, A., Gilon, C., 1991. Tyrphostins as molecular tools and potential antiproliferative drugs. Trends Pharmacol. Sci. 12, 171–174.
Mechlia, M.B., Belaid, A., Castel, G., Jallet, C., Mansfield, K.L., Fooks, A.R., Hani, K., Tordo, N., 2018. Dermaseptins as Potential Antirabies Compounds. Vaccine. https://doi.org/10.1016/j.vaccine.2018.01.066.
Moseley, G.W., Filmer, R.P., DeJesus, M.A., Jans, D.A., 2007. Nucleocytoplasmic distribution of rabies virus P-protein is regulated by phosphorylation adjacent to C-terminal nuclear import and export signals †. Biochemistry 46, 12053–12061. https://doi.org/10.1021/bi700521m.
Nikolic, J., Civas, A., Lama, Z., Lagaudrière-Gesbert, C., Blondel, D., 2016. Rabies virus infection induces the formation of stress granules closely connected to the viral factories. PLoS Pathog. 12, e1005942. https://doi.org/10.1371/journal.ppat.1005942.
Nikolic, J., Le Bars, R., Lama, Z., Scrima, N., Lagaudrière-Gesbert, C., Gaudin, Y., Blondel, D., 2017. Negri bodies are viral factories with properties of liquid organelles. Nat. Commun. 8, 58. https://doi.org/10.1038/s41467-017-00102-9.
Raghu, H., Sharma-Walia, N., Veettil, M.V., Sadagopan, S., Chandran, B., 2009. Kaposi's sarcoma-associated herpesvirus utilizes an actin polymerization-dependent macropinocytic pathway to enter human dermal microvascular endothelial and human umbilical vein endothelial cells. J. Virol. 83, 4895–4911. https://doi.org/10.1128/JVI.02498-08.
Rogée, S., Larrous, F., Jochmans, D., Ben-Khalifa, Y., Neyts, J., Bourhy, H., 2018. Pyrimethamine inhibits rabies virus replication in vitro. Antivir. Res. https://doi.org/10.1016/j.antiviral.2018.10.016.
Sandgren, K.J., Wilkinson, J., Miranda-Saksena, M., McInerney, G.M., Byth-Wilson, K., Robinson, P.J., Cunningham, A.L., 2010. A differential role for macropinocytosis in mediating entry of the two forms of vaccinia virus into dendritic cells. PLoS Pathog. 6, e1000866. https://doi.org/10.1371/journal.ppat.1000866.
Sciaky, N., Presley, J., Smith, C., Zaal, K.J.M., Cole, N., Moreira, J.E., Terasaki, M., Siggia, E., Lippincott-Schwartz, J., 1997. Golgi tubule traffic and the effects of brefeldin a visualized in living cells. J. Cell Biol. 139, 1137–1155. https://doi.org/10.1083/jcb.139.5.1137.
Soltoff, S., 2007. Rottlerin: an inappropriate and ineffective inhibitor of PKCδ. Trends Pharmacol. Sci. 28, 453–458. https://doi.org/10.1016/j.tips.2007.07.003.
Superti, F., Seganti, L., Panà, A., Orsi, N., 1985. Effect of amantadine on rhabdovirus infection. Drugs Exp. Clin. Res. 11, 69–74.
Tapia, J.A., Jensen, R.T., García-Marín, L.J., 2006. Rottlerin inhibits stimulated enzymatic secretion and several intracellular signaling transduction pathways in pancreatic acinar cells by a non-PKC-δ-dependent mechanism. Biochim. Biophys. Acta Mol. Cell Res. 1763, 25–38. https://doi.org/10.1016/j.bbamcr.2005.10.007.
Thyberg, J., 1998. Tyrphostin A9 and wortmannin perturb the Golgi complex and block proliferation of vascular smooth muscle cells. Eur. J. Cell Biol. 76, 33–42. https://doi.org/10.1016/S0171-9335(98)80015-0.
Ugolini, G., 2010. Advances in viral transneuronal tracing. J. Neurosci. Methods 194, 2–20. https://doi.org/10.1016/j.jneumeth.2009.12.001.
Ward, T.H., Polishchuk, R.S., Caplan, S., Hirschberg, K., Lippincott-Schwartz, J., 2001. Maintenance of Golgi structure and function depends on the integrity of ER export. J. Cell Biol. 155, 557–570. https://doi.org/10.1083/jcb.200107045.
Wu, X., Gong, X., Foley, H.D., Schnell, M.J., Fu, Z.F., 2002. Both viral transcription and replication are reduced when the rabies virus nucleoprotein is not phosphorylated. J. Virol. 76, 4153–4161. https://doi.org/10.1128/JVI.76.9.4153-4161.2002.
Yang, J., Koprowski, H., Dietzschold, B., Fu, Z.F., 1999. Phosphorylation of rabies virus nucleoprotein regulates viral RNA transcription and replication by modulating leader RNA encapsidation. J. Virol. 73, 1661–1664.
Yura, Y., Kusaka, J., Kondo, Y., Tsujimoto, H., Yoshida, H., Sato, M., 1995. Inhibitory effect of tyrphostin on the replication of herpes simplex virus type 1. Arch. Virol. 140, 1181–1194. https://doi.org/10.1007/BF01322745.
Zhang, D., Anantharam, V., Kanthasamy, A., Kanthasamy, A.G., 2007. Neuroprotective effect of protein kinase cδ inhibitor rottlerin in cell culture and animal models of Parkinson's disease. J. Pharmacol. Exp. Ther. 322, 913–922. https://doi.org/10.1124/jpet.107.124669.